

Time-Resolved X-Ray Scattering Studies of Layer-by-Layer Epitaxial Growth

P. H. Fuoss,⁽¹⁾ D. W. Kisker,⁽²⁾ F. J. Lamelas,⁽¹⁾ G. B. Stephenson,⁽²⁾ P. Imperatori,^{(1),(a)}
and S. Brennan⁽³⁾

⁽¹⁾*AT&T Bell Laboratories, Murray Hill, New Jersey 07974*

⁽²⁾*IBM Research Division, Yorktown Heights, New York 10598*

⁽³⁾*Stanford Synchrotron Radiation Laboratory, Stanford, California 94309*

(Received 6 January 1992)

We report the first time-resolved x-ray scattering study of the homoepitaxial growth of GaAs by organometallic vapor-phase epitaxy. The growth mode was determined to be layer-by-layer by observing ≈ 1 -Hz oscillations of the x-ray intensity from the 111 crystal truncation rod near the 110 position. We show that the spatial distribution of islands can be dynamically determined by measuring the x-ray diffuse scattering near the 110. Finally, we show that significant correlations exist between the locations of islands during layer-by-layer growth.

PACS numbers: 61.50.Cj, 68.55.Ce, 81.15.Gh

During the vapor-phase epitaxial growth of crystals, a variety of growth modes occur. At low temperatures, crystals grow via a rough, three-dimensional mode which changes to layer-by-layer growth as the temperature is raised. At even higher temperatures, step-flow growth eventually dominates [1]. The presence of layer-by-layer growth in electrochemical deposition has been known for twenty years [2]. In high-vacuum vapor-phase epitaxy (e.g., molecular-beam epitaxy, MBE), these different growth modes have been experimentally established, principally by reflection high-energy electron-diffraction (RHEED) studies, for a decade [3]. However, for a wide class of growth techniques, including chemical vapor deposition and sputter deposition, information about the growth modes is not known because high ambient pressures and/or magnetic fields preclude the use of electron diffraction techniques.

The atomic mechanisms of epitaxial growth are only crudely described by specifying the growth mode. A more complete understanding would include the mechanisms and rates of surface diffusion, growth at steps, and island nucleation. Recent scanning tunneling microscopy (STM) studies of the morphology of semiconductor surfaces produced by MBE have been analyzed to obtain information about surface diffusion [4] and growth at steps [5] which occurred during deposition. But *in situ* analysis of growth using STM is currently limited by the difficulty of measuring dynamics in the hostile growth environment.

X-ray diffraction techniques and, in particular, grazing-incidence x-ray scattering have been shown to be powerful tools for the analysis of surface structure [6]. Andrews and Cowley [7] and Robinson [8] showed that the scattering intensity is nonzero along rods which pass through bulk-allowed Bragg reflections, parallel to the macroscopic surface normal. This crystal truncation rod (CTR) intensity arises because of the abrupt termination of the crystal and can be used to characterize the surface roughness of the crystal. Vlieg *et al.* demonstrated for

slow MBE growth of germanium (2 monolayers/h) that measurements at a bulk forbidden position can show oscillations during layer-by-layer growth as complete atomic layers were grown [9]. This behavior is analogous to the commonly measured RHEED oscillations. To take advantage of the capabilities of x-ray techniques for the *in situ* study of organometallic vapor-phase epitaxial (OMVPE) growth in a high-pressure (≈ 100 Torr) ambient of H₂, special techniques and equipment have been developed by Fuoss *et al.* [10].

Using time-resolved versions of these techniques, we have studied the nature of GaAs growth in an OMVPE reactor under conditions approximating those used to produce high-quality semiconductor devices. We report here results showing that layer-by-layer growth occurs over a range of OMVPE growth conditions. We also report measurements of time-dependent diffuse scattering which give information about the spatial distribution of islands during layer-by-layer growth. We obtain values for island nucleation density as a function of temperature which are consistent with the crossover between layer-by-layer and step-flow growth modes. Our results also show that correlations exist between the locations of islands during layer-by-layer growth.

The experimental requirements for these measurements are stringent. The specially constructed OMVPE reactor and diffractometer in which high-quality semiconductor films can be grown while simultaneously allowing the diffraction of x rays from the surface has been previously described [11]. This reference also discusses in detail the scattering geometry used for these experiments. A very bright synchrotron radiation source is also required since we wish to perform time-resolved measurements from a two-dimensional film with a time resolution of < 0.1 s. The x-ray source used for these experiments is beam line 10-2 at the Stanford Synchrotron Radiation Laboratory. BL 10-2 is driven by a 15-period hybrid wiggler whose radiation is focused by a bent-cylinder mirror. A double-crystal, parallel-setting Si(111) monochromator

was used to select 10300-eV photons. For the time-resolved measurements, the synchrotron beam was typically collimated with a 2.8-mrad horizontal slit in front of the mirror and by 4.2 mm \times 0.6 mm entrance slits in front of the diffractometer. A photon flux of $\approx 5 \times 10^{16}$ photons/s was measured after these slits under the typical operating conditions of 35 mA and a wiggler field of 1.4 T. The scattered beam was detected through ± 2.0 -mm vertical slits 500 mm from the sample (normal to the scattering plane) and by a 10-mrad Soller slit in the horizontal scattering plane. With these settings, the in-plane resolution of the instrument at the 110 was 0.008 \AA^{-1} perpendicular and 0.016 \AA^{-1} parallel to the scattering vector. Thus, 800- \AA correlations could be resolved in rocking scans and 400- \AA correlations in radial scans.

The substrates used for the growth described in this paper were GaAs(001) wafers 25 mm in diameter and 1 mm thick. The miscut of the substrate used for these experiments was checked by measuring the CTR splitting and was found to be 0.046 $^\circ$ towards the [1 $\bar{1}$ 0] direction. The substrates were solvent cleaned and then etched in 15:3:1 H₂O:NH₄OH:H₂O₂ for 2 min followed by (NH₄)₂S for 1 min. Following this surface preparation, the sample was annealed at 600 $^\circ$ C in flowing tertiarybutylarsine (TBAs) and H₂ at 50 Torr until the surface was smooth as indicated by a sharp and intense 110 CTR. Typical flows were 1 standard liter per minute (slpm) H₂ and 150 μ mol/min TBAs through the nozzle with 5.65 slpm of H₂ flowing through the window purge system.

In this paper, we will describe the time dependence of the intensity and transverse shape of a CTR during GaAs growth. Figure 1 shows the CTR intensity at (1,1,0.05) obtained during a typical growth run at 540 $^\circ$ C. Under constant TBAs flow of 150 μ mol/min, a trimethylgallium (TMG) flow of 3.8 μ mol/min is turned on 10 s into the experiment. The dashed line represents the TMG partial pressure calculated from the reactor response time. As TMG is introduced into the reactor, oscillations corre-

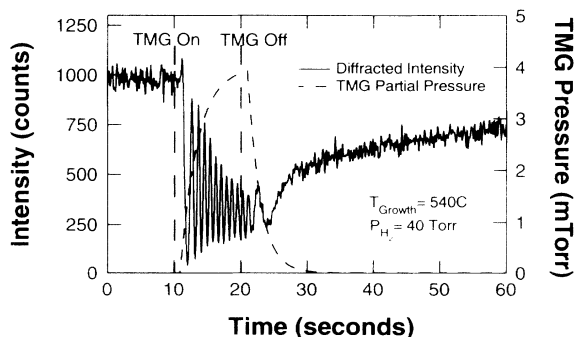


FIG. 1. X-ray intensity oscillations of the (1,1,0.05) diffraction peak during a typical growth run at 540 $^\circ$ C. The dashed line shows the partial pressure of TMG reaching a peak of 4 mTorr. The partial pressure of TBAs was a constant 150 mTorr and the total reactor pressure was 50 Torr. Twelve atomic bilayers or 34 \AA of GaAs were grown in this cycle.

sponding to the growth of atomic bilayers are clearly seen in the data. 20 s into the measurement the TMG flow is turned off. As the TMG is purged from the reactor, two more layers of GaAs are grown and the intensity is left at a fraction of its initial value. The CTR intensity fully recovers to its initial value within 5 min. Since the intensity of the CTR near the 110 position can be directly related to the fractional completion of the last atomic bilayer of the crystal (being weaker when the bilayer is half completed and stronger when it is fully completed [6-9]), the oscillations shown in Fig. 1 are clear and convincing evidence that layer-by-layer growth is occurring during this OMVPE process.

The temperature dependence of this process has been studied in some detail. Figure 2 shows data taken on this sample at four temperatures but at constant partial pressure. At 520 $^\circ$ C the growth is significantly slower than at higher temperatures showing that the growth rate is not limited by mass transport but rather by reaction kinetics, most likely the decomposition rate of the organometallics. After the TMG flow is turned off, the CTR intensity recovers as the remaining bilayer-high islands coarsen. Although the coarsening is generally faster at higher temperature, consistent with faster surface diffusion and a higher density of mobile surface species, the time to recover depends strongly on the fractional completion of the last bilayer grown. At all temperatures we observe a damping of the CTR oscillations during growth. While several aspects of these curves depend on temperature, the asymptotic value of the CTR intensity as the oscillations are damped is relatively insensitive to temperature. The asymptotic value of $\approx \frac{1}{3}$ of the initial value and the

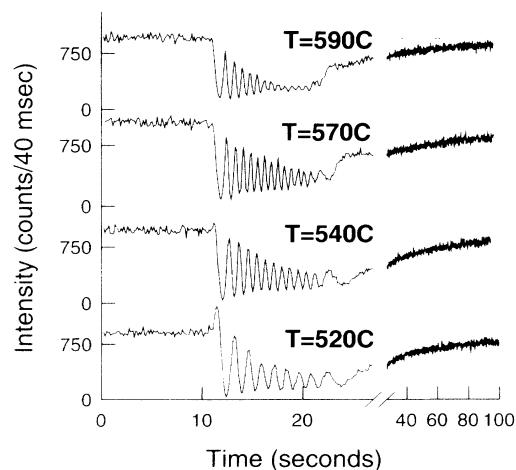


FIG. 2. X-ray intensity oscillations of the (1,1,0.05) diffraction peak at the series of temperatures discussed in this paper. Note the qualitative change in the onset of growth between 520 and 540 $^\circ$ C. At 520 $^\circ$ C there is a consistent increase in the diffracted signal as growth starts while at higher temperatures the signal almost always decreases as growth starts. Note also that the growth rate is significantly slower at 520 $^\circ$ C.

fact that the minima of the oscillations increase with time argue that the damping is caused by nonuniform growth [12]. A nonuniformity of $\approx 2\%$ over the sampled area of $7\text{ mm}\times 4\text{ mm}$ would explain the results for growth at 540°C . The apparent decrease in uniformity for growth at 520°C may be explained by temperature gradients across the sample since the growth rate at low temperatures is a sensitive function of temperature. At 590°C the growth mode is changing from layer-by-layer to step flow and the explanation of the decay may be more complex.

The spatial distribution of islands and the density of nucleation can be studied by examining the in-plane diffuse scattering around the CTR as a function of time. As in classical small-angle scattering [13], such diffuse scattering arises from the islands found in a partially completed atomic bilayer. Figure 3 shows a contour plot of the data obtained during the first oscillation of growth at 540°C . These data were obtained by carrying out a sequence of identical 15-s growth runs and monitoring the intensity at different wave vectors during each run. Wave vectors along the $[1\bar{1}0]$ direction through the $(1,1,0.5)$ position were selected; the data are plotted in terms of the transverse component $\Delta q_t = q_{(1,1,0.05)} \sin(\theta - \theta_{(1,1,0.05)})$. Near the time when the scattering at $\Delta q_t = 0$ is minimum, there is a maximum in the diffuse scattering at Δq_t above 0.01 \AA^{-1} . This is the time at which the surface is 50% covered with islands.

The dependence of the diffuse scattering on Δq_t reflects the instantaneous spatial distribution of islands in the $[1\bar{1}0]$ direction. For the 50% covered surface, there is a broad shoulder in the diffuse scattering with a weak but well-defined maximum at $\Delta q_t = 0.02\text{ \AA}^{-1}$. As in the case of a concentrated suspension of particles, the presence of a maximum in the diffuse scattering shows that the positions of the islands are strongly correlated. To an accuracy

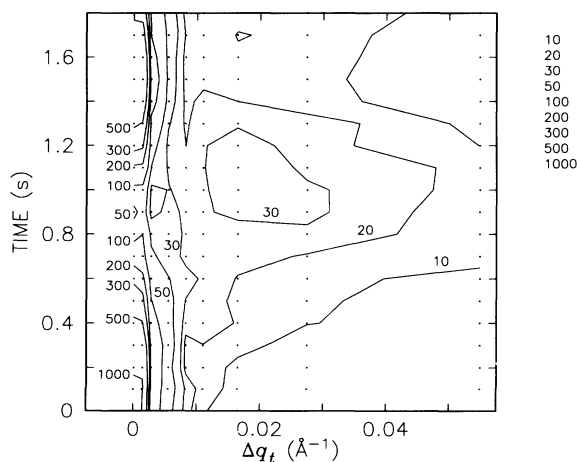


FIG. 3. The diffuse scattering associated with the $(1,1,0.05)$ diffraction peak during the first cycle of growth. These data are a composite of nine growth runs at different, fixed values of Δq_t .

of 50%, the position of the maximum can be used to determine the island spacing on the surface through the relationship $L \approx 2\pi/\Delta q_t^{\text{max}}$ [13]. This spacing, $\approx 300\text{ \AA}$, is directly related to the density of nucleation at 540°C .

It is informative to estimate the temperature dependence of the nucleation density, since it is expected to be controlled by a competition between surface diffusion and deposition rate. Figure 4 shows the diffuse scattering at 50% coverage for each of the temperatures in Fig. 2. At 520°C the diffuse scattering extends to Δq_t above 0.03 \AA^{-1} . At 540°C there is a weak peak at $\Delta q_t = 0.02\text{ \AA}^{-1}$. At 570° , this peak occurs at $\Delta q_t = 0.014\text{ \AA}^{-1}$. At 590°C , it has merged with the sharp peak at $\Delta q_t = 0$. Estimates of the island spacing in the $[1\bar{1}0]$ direction are $L_{520^\circ\text{C}} < 200\text{ \AA}$, $L_{540^\circ\text{C}} \approx 300\text{ \AA}$, $L_{570^\circ\text{C}} \approx 450\text{ \AA}$, and $L_{590^\circ\text{C}} > 800\text{ \AA}$. This trend in island spacing is consistent with the decrease in nucleation density expected as the surface diffusion length increases at higher temperature, at constant deposition rate. A comparison of these sizes to the terrace width of $\approx 3500\text{ \AA}$ along the $[1\bar{1}0]$ direction would suggest a crossover from layer-by-layer to step-flow growth at $\approx 630^\circ\text{C}$. Measurements at 625°C show that the oscillations are nearly gone, indicating a crossover to step-flow growth in agreement with this prediction.

Anisotropy of island morphology was investigated by making similar measurements of the diffuse scattering in the $[110]$ direction near the $1\bar{1}0$ CTR during growth at 560°C . The increase in the diffuse intensity in this direction was dramatically smaller, with no increase at transverse wave numbers above 0.02 \AA^{-1} . This indicates that the island shape during layer-by-layer growth is anisotropic, with the island spacing at 50% coverage at least a factor of 3 larger in the $[110]$ direction than the $[1\bar{1}0]$

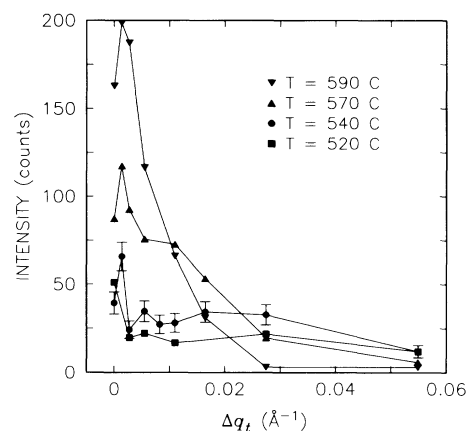


FIG. 4. The diffuse scattering associated with the $(1,1,0.05)$ diffraction peak at the minimum (in time) of the on-axis intensity for four different temperatures. The data for 540°C is the 0.9-s curve from Fig. 3. Note the weak maximum in each data set moves to lower Δq_t as the temperature and diffusion coefficient is raised.

direction. The direction of this anisotropy is opposite to that found in an STM study of samples quenched during MBE growth [5]. Such differences are not surprising since the surface reconstructions we find present in the OMVPE environment [14] differ significantly from those found in the MBE study. This provides evidence that the mechanisms of surface diffusion and step motion which determine growth anisotropy are qualitatively different during OMVPE from those during MBE.

In summary, our *in situ*, time-resolved x-ray analysis has shown that layer-by-layer growth occurs during OMVPE of GaAs using TBAs and TMG as the source materials. At a growth rate of ≈ 1 bilayer/s, layer-by-layer growth occurred between 520°C and 600°C. Analysis of the diffuse x-ray scattering revealed average island spacings at 50% coverage ranging from < 200 Å at 520°C to > 800 Å at 590°C. In addition, these islands are not randomly nucleated but have positions which are correlated. This result is consistent with the existence of a denuded zone inhibiting nucleation surrounding each island.

These results clearly show that analysis of the diffuse scattering associated with x-ray intensity oscillations is a powerful tool for the microscopic characterization of growth. Future opportunities include measurement of absolute nucleation rates and the quantitative determination of the shape and size distributions of islands during growth. While important in itself, that will also allow the determination of the anisotropy of diffusion coefficients, and may lend some insight into the actual attachment kinetics at step edges. Further, the anisotropic nature of the nucleation and growth process may explain the wide variation in heterojunction interface abruptness measured by techniques which are sensitive to different length scales. Finally, the understanding of the details of the relationship between surface atomic arrangements due to reconstructions and the nucleation and growth kinetics will enhance our understanding of the chemical vapor deposition process.

We would like to thank A. Fischer-Colbrie, G. H. Gilmer, M. H. Grabow, R. M. Lum, and I. K. Robinson for helpful discussions and suggestions. The help of K. L. Tokuda was invaluable. These experiments were per-

formed at the Stanford Synchrotron Radiation Laboratory which is supported by the Department of Energy, Division of Chemical Sciences. Support for one of us (S.B.) is provided by the Department of Energy, Office of Basic Energy Sciences.

(a)Permanent address: CNR-Istituto di Teoria e Struttura Elettronica, Area Della Ricerca Di Roma, 00016 Monterotondo Staz, Italy.

- [1] G. H. Gilmer, *J. Cryst. Growth* **49**, 465 (1980).
- [2] V. Bostanov, R. Roussinova, and E. Budevski, *J. Electrochem. Soc.* **119**, 1346 (1972).
- [3] J. H. Neave, B. A. Joyce, P. J. Dobson, and N. Norton, *Appl. Phys. A* **31**, 1 (1983).
- [4] Y. W. Mo, J. Kleiner, M. B. Webb, and M. G. Lagally, *Phys. Rev. Lett.* **66**, 1998 (1991).
- [5] E. J. Heller and M. G. Lagally, *Appl. Phys. Lett.* **60**, 2675 (1992).
- [6] P. H. Fuoss and S. Brennan, *Annu. Rev. Mater. Sci.* **20**, 365 (1990), and references therein.
- [7] S. R. Andrews and R. A. Cowley, *J. Phys. C* **18**, 6427 (1985).
- [8] I. K. Robinson, *Phys. Rev. B* **33**, 3830 (1986).
- [9] E. Vlieg, A. W. Denier van der Gon, J. F. van der Veen, J. E. MacDonald, and C. Norris, *Phys. Rev. Lett.* **61**, 2241 (1988).
- [10] P. H. Fuoss, D. W. Kisker, G. Renaud, K. L. Tokuda, S. Brennan, and J. L. Kahn, *Phys. Rev. Lett.* **63**, 2389 (1989); D. W. Kisker, P. H. Fuoss, K. L. Tokuda, G. Renaud, S. Brennan, and J. L. Kahn, *Appl. Phys. Lett.* **56**, 2025 (1990).
- [11] S. Brennan, P. H. Fuoss, J. L. Kahn, and D. W. Kisker, *Nucl. Instrum. Methods Phys. Res., Sect. A* **291**, 86 (1990).
- [12] M. Henzler, in *Reflection High-Energy Electron Diffraction and Reflection Electron Imaging of Surfaces*, edited by P. K. Larsen and P. J. Dobson (Plenum, New York, 1988), pp. 193-199.
- [13] A. Guinier and G. Fournet, *Small-Angle Scattering of X-Rays*, translated by C. B. Walker (Wiley, London, 1955).
- [14] F. J. Lamellas, P. H. Fuoss, P. Imperatori, D. W. Kisker, G. B. Stephenson, and S. Brennan, *Appl. Phys. Lett.* **60**, 2610 (1992).